

Angular distributions for ^{14}C , $^{26}\text{Mg}(\pi^+, \pi^-)$

R. Gilman, H. T. Fortune, and J. D. Zumbro
University of Pennsylvania, Philadelphia, Pennsylvania 19104

Peter A. Seidl and C. Fred Moore
University of Texas at Austin, Austin, Texas 78712

C. L. Morris
Los Alamos National Laboratory, Los Alamos, New Mexico 87545

J. A. Faucett and G. R. Burlison
New Mexico State University, Las Cruces, New Mexico 88003

S. Mordechai*
University of Pennsylvania, Philadelphia, Pennsylvania 19104
and University of Texas at Austin, Austin, Texas 78712

Kalvir S. Dhuga†
University of Pennsylvania, Philadelphia, Pennsylvania 19104
and New Mexico State University, Las Cruces, New Mexico 88003

(Received 2 August 1985)

Cross sections at $\theta = 5^\circ$ (lab) were obtained at seven energies for $^{14}\text{C}(\pi^+, \pi^-)^{14}\text{O}(\text{g.s.})$ and at four energies for $^{26}\text{Mg}(\pi^+, \pi^-)^{26}\text{Si}(\text{g.s.})$. Angular distributions have been measured for both reactions at energies of 140 and 200 MeV. The results are compared to previous angular distributions at other energies on these two nuclei, and to a series of angular distributions measured for $^{18}\text{O}(\pi^+, \pi^-)$.

The inadequacy of lowest-order theories of pion double charge exchange (DCX) to the double-isobaric-analog state (DIAS) has long been known. The angular-distribution anomaly is the presence of “nondiffractive” forward minima exhibited at 164 MeV (whereas 292-MeV angular distributions appear simply diffractive).¹⁻³ The excitation-function anomaly is the existence of peaks in the cross section at energies below the Δ resonance^{1,3} [or, e.g., the large cross section observed for $^{14}\text{C}(\pi^+, \pi^-)^{14}\text{O}(\text{g.s.})$ at 50 MeV].⁴ In contrast, lowest-order calculations typically predict a monotonic rise in the cross section between ~ 50 and ~ 300 MeV.⁵

This situation has prompted a number of investigations of various additional reaction mechanisms and higher-order optical potentials. At present, the theoretical results that best reproduce the data are the higher-order optical-potential descriptions of Liu⁶ and of Johnson and Siciliano.⁷ Various calculations that have invoked additional reaction mechanisms have, quite simply, failed. However, we note that recent calculations of a nonsequential reaction mechanism show promise of being an explanation for nonanalog DCX.⁸ Thus, the contributions of this mechanism to DIAS DCX need to be closely examined.

Given the success of the two theories at “explaining” the angular-distribution anomaly, it was decided to investigate the energy dependence of DIAS angular-distribution shapes. The investigation would enable comparisons between different theories and data at several energies. Measurements for $^{18}\text{O}(\pi^+, \pi^-)^{18}\text{Ne}(\text{g.s.})$ were reported in a recent Letter.⁹ The ^{18}O angular distributions exhibited well-defined forward minima for energies at and below 180 MeV, an angular distribution at 200 MeV had constant large-angle cross sections, and diffractive angular distribu-

tions were measured at and above 230 MeV. It was speculated,⁹ given the similar shapes for ^{18}O at 200 MeV and ^{14}C at 164 MeV,³ that the transition from the diffractive energy region to the forward-minimum region occurs at an energy roughly 40 MeV higher in ^{18}O than in ^{14}C .

The ^{18}O target had been picked because it has the highest DCX count rate of any readily available target. We report here on the measurement of angular distributions at two additional energies for both ^{14}C , $^{26}\text{Mg}(\pi^+, \pi^-)^{14}\text{O}(\text{g.s.})$, $^{26}\text{Si}(\text{g.s.})$. The data presented here are complementary to those on ^{18}O , so that theoretical comparisons would not rest on results for a single nucleus, and so that general reaction mechanism effects could be identified.

The data were measured at the Energetic Pion Channel and Spectrometer (EPICS) at the Clinton P. Anderson Meson Physics Facility (LAMPF). Descriptions of pertinent experimental details can be found in Refs. 3 and 9. The angular range of the small-angle DCX setup was limited to scattering angles less than about 41° . A strip target of ^{14}C and ^{26}Mg similar to that of Ref. 3 was used, except that the target consisted of two strips of ^{26}Mg positioned above and below a central strip of ^{14}C . Thus, the ^{26}Mg areal density was half that of Ref. 3, but the amount of material in the beam was the same. Also, the ^{14}C target powder had been repacked from nickel cells used in the earlier experiment into copper cells of the same volume. There was almost no change in the areal density of the ^{14}C . Given the relative amounts of material and the approximate mass dependence of DIAS DCX,

$$d\sigma/d\Omega \sim (N-Z)(N-Z-1)A^{-10/3},$$

it was expected that the ^{14}C count rate would be three to

TABLE I. $^{14}\text{C}(\pi^+, \pi^-)^{14}\text{O}(\text{g.s.})$ cross sections measured in this work.

T_π (MeV)	θ_{lab} (deg)	$d\sigma/d\Omega_{\text{lab}}$ ($\mu\text{b}/\text{sr}$)
80.0	5.5	0.962 ± 0.340
100.0	5.5	0.614 ± 0.194
140.0	5.5	1.556 ± 0.271
	15.5	0.477 ± 0.109
	20.5	0.330 ± 0.110
	25.5	0.135 ± 0.067
	30.5	< 0.045
	35.5	0.172 ± 0.065
	40.5	0.115 ± 0.058
164.0	5.5	1.948 ± 0.355
200.0	5.5	2.973 ± 0.489
	15.5	1.849 ± 0.344
	25.5	0.449 ± 0.098
	30.5	0.202 ± 0.082
	35.5	0.157 ± 0.052
	40.5	0.167 ± 0.059
230.0	5.5	4.823 ± 0.645
292.0	5.0	4.701 ± 0.555

four times larger than that for ^{26}Mg . In general, however, run times were determined by the ^{14}C measurements, resulting in statistically poor determinations of the ^{26}Mg cross sections.

The cross sections measured for ^{14}C and ^{26}Mg are listed in Tables I and II. The 5° excitation functions are plotted in Fig. 1. The most striking feature is the appearance that the new ^{14}C data are systematically larger than the old data (whereas the ^{26}Mg overlap is adequate). Between 130 and 300 MeV, the new data average 1.4 times larger than the old data. The statistical uncertainties of the data points are roughly 15%, and the estimated uncertainty in the overall normalization is $\sim 7\%$ for each data set. Thus, there is an inconsistency between the two data sets. Unfortunately, after a careful examination of the two data sets, we see no reasons to believe there are errors in the normalizations of either data set.

Absolute normalization of the cross sections is performed relative to hydrogen scattering,

$$\sigma_{\text{DCX}} = \frac{2}{14} \rho_{\text{CH}_2} \frac{\sigma_{\text{H}}}{Y_{\text{H}}} \frac{A_{\text{DCX}}}{\rho_{\text{DCX}}} Y_{\text{DCX}} .$$

The factor Y is the yield for the reaction, the number of counts per unit of beam corrected for, e.g., detector efficiencies, pion survival fractions, and computer live time. Target thicknesses and hydrogen cross sections were consistent for the two experiments. The full-target CH_2 normalization factor ($\rho\sigma/Y$) is $\sim 40\%$ larger (independent of beam energy) for the present data set than for the earlier data set. This is not unusual, however, as changes in, for example, beam monitor calibrations, pion channel configuration, and chamber gas mixtures can affect the absolute magnitude of these numbers. The good overlap between new and old ^{18}O (Ref. 9) data, for example, uses normalization factors that differ by $\sim 20\%$.

Target cuts were consistent for the two reactions. In both cases, the ^{14}C target was centered in the beam and contributed about one-third of the full target acceptance. There

TABLE II. $^{26}\text{Mg}(\pi^+, \pi^-)^{26}\text{Si}(\text{g.s.})$ cross sections measured in this work.

T_π (MeV)	θ_{lab} (deg)	$d\sigma/d\Omega_{\text{lab}}$ ($\mu\text{b}/\text{sr}$)
140.0	5.5	0.324 ± 0.087
	15.5	0.099 ± 0.034
	20.5	0.018 ± 0.018
	25.5	< 0.017
	30.5	0.110 ± 0.049
	35.5	0.157 ± 0.043
	40.5	0.113 ± 0.040
164.0	5.5	0.482 ± 0.124
200.0	5.5	0.152 ± 0.077
	15.5	0.030 ± 0.030
	25.5	0.030 ± 0.018
	30.5	0.032 ± 0.023
	35.5	0.041 ± 0.019
	40.5	< 0.010
230.0	5.5	0.423 ± 0.133

is no indication of any loss of DCX counts in the earlier data due to too tight target cuts. The most likely error in the calculation of correction factors in the yield would be an underestimate of detection efficiencies (and a too large cross section), if these were calculated for many events that were not pions. The calculated corrections for the recent data are all about as expected, however.

Cross sections for other targets measured with the ^{14}C show reasonable overlap. There is ^{26}Mg data presented here

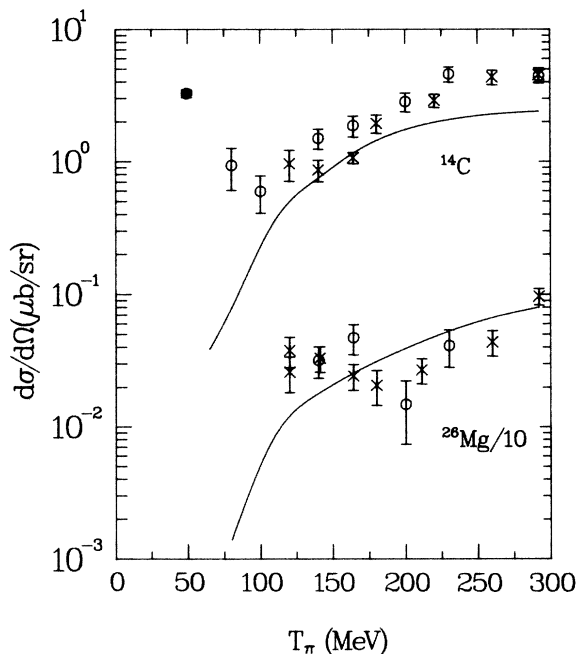


FIG. 1. Excitation functions for ^{14}C , $^{26}\text{Mg}(\pi^+, \pi^-)$ at $\theta = 5^\circ$ (lab). Solid lines are calculations with the computer code PIESDEX (Ref. 11) and Skyrme III densities for ^{14}C and ^{26}Mg . Data points from this work are marked by circles. Old data (marked by crosses) are from Ref. 3. The ^{14}C datum at 50 MeV (filled circle) is from Ref. 4.

and ^{13}C and ^{56}Fe data as well. None of these measurements show any overlap problems. While this would seem to indicate problems with the ^{14}C target repacking, extreme differences (e.g., a 1-cm gap in the center of the target) in the packing of the two sets of ^{14}C target cells would result in systematic effects of only $\sim 20\%$ (because of the EPICS beam profile). A recent analysis of the ^{14}C target has shown the presence of some impurities in the target that were not included in the analysis of the earlier data. This results in a correction to those data, increasing the cross sections by 6.3% over the values reported in Ref. 3; but that correction is already included in all plots and numbers in this article. This is not sufficient to eliminate the inconsistency. We conclude that we do not understand the inconsistency in the two data sets.

Given the large ^{14}C cross sections measured at 50 MeV,⁴ it was desired to measure as close as possible to an overlap point. The EPICS data show no evidence for an increasing lower-energy cross section except for perhaps at the lowest-energy measurement at 80 MeV. The excitation function therefore must exhibit a dramatic increase in cross section between 80 and 50 MeV. This factor of 4 increase in such a short energy interval is among the most rapid energy dependencies observed in pion scattering. The reaction mechanism underlying the large 50-MeV cross sections is not, however, understood.¹⁰ In addition, no data have been published for other nuclei at energies below 80 MeV.

The measured angular distributions for ^{14}C and ^{26}Mg are shown in Figs. 2 and 3. Also shown are previous measurements, and lowest-order DCX calculations performed with the code PIESEX.¹¹ Some features should be noted. The ^{14}C angular distribution at 200 MeV is close to diffractive.

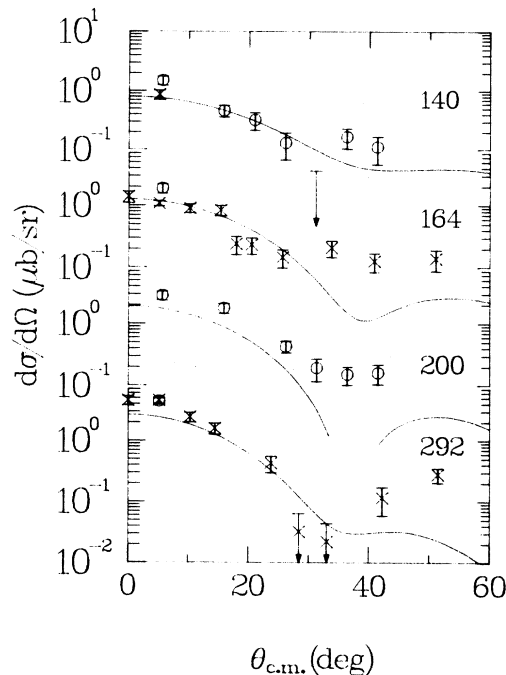


FIG. 2. Angular distributions at four energies for $^{14}\text{C}(\pi^+, \pi^-)$. Solid lines are calculations with the computer code PIESEX (Ref. 11) and a Skyrme III density for ^{14}C . Data points from this work are marked by circles. Old data (marked by crosses) are from Ref. 3.

The agreement between the shape of the calculation and the shape of the data between 0° and 30° is very good. In contrast, for ^{18}O at this energy,⁹ a transitional shape was observed that had constant cross sections at all angles larger than 15° . While the 200-MeV ^{26}Mg angular distribution is consistent with the transitional shape, the statistics are too poor to make a definitive judgment. At 140 MeV, both the ^{18}O angular distribution⁹ and the new ^{26}Mg angular distribution exhibit well-defined forward minima.

The 140-MeV angular distribution for ^{14}C does not exhibit a well-defined shape. We would not expect a diffractive "minimum" near 40° , as indicated in the calculation in Fig. 2, as all angular distributions for ^{18}O and ^{26}Mg between 100 and 200 MeV exhibit well-defined forward minima. (Of course, the deep minima predicted on resonance, ~ 180 MeV, are washed out in the calculations at this lower energy.) By this standard, however, the 164-MeV ^{14}C angular distribution is also anomalous. If the speculation about a transitional energy region⁹ is correct, we might expect at 140 MeV a well-defined forward minimum near 30° , or an angular distribution that is flat for $\theta \geq 25^\circ$, similar to the 164-MeV ^{14}C result. Although the data are more consistent with a 30° minimum than with either a 40° minimum or a flattened angular distribution, the results are not definitive. We tentatively conclude that the new data support the speculation that the transition region is at about 40-MeV lower energy for ^{14}C than for ^{18}O , whereas the ^{26}Mg results indicate a transition at an energy close to that for ^{18}O .

Although the Skyrme densities used in these calculations result in reasonable agreement with the position of the minima of angular distributions at higher energies, they do not provide an adequate description of the angular-

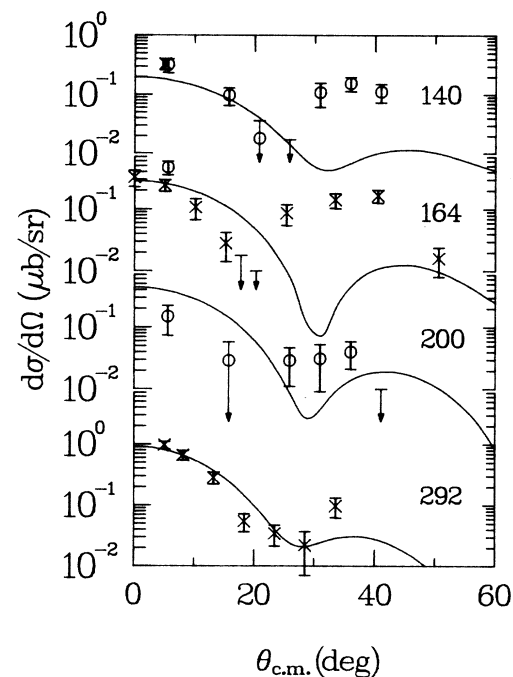


FIG. 3. Angular distributions for $^{26}\text{Mg}(\pi^+, \pi^-)$ at four energies. Solid lines are calculations with the computer code PIESEX (Ref. 11) and a Skyrme III density for ^{26}Mg . Data points from this work are marked by circles. Old data (marked by crosses) are from Ref. 3.

distribution shape. It should be noted, however, that calculations^{5,6} of DCX at 292 MeV in general underestimate cross sections out beyond the first minimum. Thus, this failure may be due more to inadequacies in the reaction-mechanism calculations at high momentum transfer than to inadequacies in the densities.¹²

The similarity of angular-distribution behavior for ¹⁸O and ²⁶Mg, and the difference for ¹⁴C, is reflected in the excitation functions for the three nuclei. For ¹⁸O, there is a minimum in the excitation function at about 180 MeV, and a peak near 140 MeV for which the cross sections are nearly as large as at 292 MeV. The ¹⁴C excitation function, which clearly exhibits a monotonic increase with energy above 140 MeV (despite the ambiguities in the absolute normalization), is obviously different. The ²⁶Mg shape is much more similar to that for ¹⁸O, although the degree to which the excitation function peaks near 140 MeV is obscured by the poor statistics. The ratios of cross sections at 140 to those at 180 MeV are 0.5 ± 0.1 for ¹⁴C, 2.2 ± 0.4 for ¹⁸O, and 1.6 ± 0.5 for ²⁶Mg. Connections between the peaking of the excitation functions and the nondiffractive forward minima are expected in the two-amplitude model approach to

DCX,¹³ in which a second nonsequential reaction mechanism would result in both phenomena. Work on a microscopic theory for this model is underway.¹⁴

In conclusion, measurements of DCX angular distributions on ¹⁴C and ²⁶Mg confirm earlier observations on ¹⁸O. There exist energy ranges near the Δ resonance in which angular distributions exhibit forward minima, energy ranges between 200 (or 230) and 300 MeV for which angular distributions are simply diffractive, and a transition region between these two ranges. The extent of these ranges depends on the target nucleus in a way that is not presently understood.

The authors thank Helmut W. Baer for the loan of the ¹⁴C target, and for his assistance in target preparation. We would also like to thank K. K. Seth for the loan of the ²⁶Mg target. We also thank J. van Dyke and Barolin Romero for their assistance in target vacuum tests. This work has been supported in part by the U.S. Department of Energy, the National Science Foundation, and the Robert A. Welch Foundation.

*Permanent address: Ben-Gurion University of the Negev, Beer-Sheva, Israel.

†Present address: New Mexico State University, Las Cruces, NM 88003.

¹S. J. Greene *et al.*, Phys. Lett. **88B**, 62 (1979).

²K. K. Seth *et al.*, Phys. Rev. Lett. **43**, 1574 (1979); **45**, 147 (1980).

³Peter A. Seidl *et al.*, Phys. Rev. C **30**, 973 (1984); S. J. Greene *et al.*, *ibid.* **25**, 927 (1982).

⁴M. J. Leitch *et al.*, Phys. Rev. Lett. **54**, 1482 (1985); I. Navon *et al.*, *ibid.* **52**, 105 (1984).

⁵Gerald A. Miller, Phys. Rev. C **24**, 221 (1981).

⁶L. C. Liu, Phys. Rev. C **27**, 1611 (1983).

⁷Mikkel B. Johnson and E. R. Siciliano, Phys. Rev. C **27**, 730

(1983); Steven J. Greene *et al.*, *ibid.* **30**, 2003 (1984).

⁸R. Gilman *et al.*, Phys. Rev. C **32**, 349 (1985).

⁹Peter A. Seidl *et al.*, Phys. Lett. **154B**, 255 (1985).

¹⁰See, e.g., T. Karapiperis or W. Gibbs, in Proceedings of the LAMPF Workshop on Pion Double Charge Exchange, Los Alamos, January 12–14, 1985, Los Alamos National Laboratory Report No. LA-10550-C, 1985.

¹¹Mikkel B. Johnson and E. R. Siciliano, Phys. Rev. C **27**, 1647 (1983).

¹²L. C. Liu (private communication).

¹³R. Gilman *et al.*, Nucl. Phys. **A432**, 610 (1985); S. J. Greene *et al.*, Phys. Rev. C **25**, 924 (1982).

¹⁴A. Wirzba *et al.* (unpublished).